Carbohydrate Polymers 98 (2013) 842–853

Contents lists available at SciVerse ScienceDirect

Carbohydrate Polymers

journal homepage: www.elsevier.com/locate/carbpol

# Starch-based extruded cereals enriched in fibers: A behavior of composite solid foams

Hélène Chanvrier*, Fabrice Desbois, Fabienne Perotti, Claire Salzmann, Sophie Chassagne, Jean-Claude Gumy, Imre Blank

*Nestec S.A.—PTC Orbe, Route de Chavornay 3, 1350 ORBE, Switzerland*

ARTICLE INFO

*Article history:*
Received 8 January 2013
Received in revised form 1 July 2013
Accepted 2 July 2013
Available online 11 July 2013

*Keywords:*
Extruded cereals
Structure
Solid foams
Mechanical properties
Matrix–particles materials

ABSTRACT

Extruded cereals mainly composed of starch and enriched in fibers were produced with two types of base recipes: (i) one recipe mainly composed of wheat flour and (ii) one recipe mainly composed of corn and soya flours. The addition of fibers was performed through the use of oat bran concentrate or wheat bran, up to 32% of the recipe. The structure of the extrudates, assessed by X-ray tomography, pointed out the decrease of porosity and of mean cells size with the increase of the total dietary fibers content of the recipe. The hardness of the products, i.e. the maximum stress determined by a compression test, was linked to their porosity. The Gibson–Ashby relationship could be applied and the fit was even improved when considering the walls of the solid foam as composite materials. Fibers and proteins can be indeed considered as particles dispersed in the starchy phase. This work thus shows the impact of the structure of the extrudates on their mechanical properties. The structure is taken into account at different length scales; at the level of the porous structure and at the level of the phase of the main biopolymers present in the recipe (starch, proteins and fibers). The mechanical behavior of these products is then discussed according to their characteristics of composite solid foams.



## 1. Introduction

The European InsideFood project, combining a consortium of 12 European partners, aimed at studying the structure of different types of food at different length scales, the final objective being to develop on-line sensors. In this purpose, there was a need to firstly develop cutting-edge analytical methods and secondly to better understand the selected food products through the ranges of structures that were possible to produce. The InsideFood project focused on food products such as gels, foamy gels and extruded cereals. Since cereal-based products with high amount of fibers are of interest for nutritional purposes and health benefits (Topping, 2007; Vitaglione, Napolitano, & Fogliano, 2008; Murphy et al., 2012), starch-based extruded cereals supplemented in fibers were chosen as a food system to develop methods and deepen the knowledge on the fibers effect.

Extrusion-cooking is a food process that is widely used in the food industry for the production of cereal products, allowing the shaping as well as the texturization of cooked cereal flours. Starchy extruded cereal products are usually porous and aerated due to the expansion process that occurs at the end of the die. This expansion is governed by the water vaporization, which is the driving force of this phenomenon, but also by the rheological properties of the molten products before reaching their solidification (Fan, Mitchell, & Blanshard, 1994; Launay, 1994; Della Valle, Vergnes, Colonna, & Patria, 1997). The rheological properties, and more specifically the elongational viscosity, create a resistance towards the expansion, and are assumed to be dependent on the composition of the products and on the presence of fillers (Xanthos, 2005). Indeed, any major ingredient, such as added proteins, fibers or sugars, strongly modifies the viscosity of the melt in the extruder. The glass transition temperature ($T_g$) of the products is also a key attribute; the higher the $T_g$, the quicker the solidification of the structure during cooling, thus avoiding any structure collapse. The acquisition of the porous structure of extruded cereals is thus submitted to many factors, and the fibers content is one of them. The impact of fibers on the final extruded products has been widely reported in literature, and it is known that fibers are detrimental to the expansion (Brennan, Monro, & Brennan, 2008; Robin, Dubois, Pineau, Schuchmann, & Palzer, 2011a; Robin, Dubois, Curti, Schuchmann, & Palzer, 2011b). But fibers may act in a different way according to their origins and chemistry (Yanniotis, Petraki, & Soumpasi, 2007).

Some textural sensory attributes such as hardness depend on the mechanical properties of the extruded cereals. According to the Gibson and Ashby relationship applicable for cellular solids (Gibson and Ashby, 1997), the stress at rupture of the foam can be related to the density of the foam, characterizing the aeration of the solid foam: $\sigma^*/\sigma_s = C(\rho^*/\rho_s)^n$, with $C$, a constant, $\sigma^*$, the stress at rupture

* Corresponding author. Tel.: +41 24 442 71 11; fax: +41 24 442 74 44.
*E-mail address:* helene.chanvrier@rdor.nestle.com (H. Chanvrier).

0144-8617/$ – see front matter 
http://dx.doi.org/10.1016/j.carbpol.2013.07.005

of the solid foam, $\sigma_s$, the stress at rupture of the dense matrix, i.e. the intrinsic materials, $\rho^*$ the density of the foams, $\rho_s$, the density of the dense matrix. This relationship has been previously applied to cereal-based solid food products (Warburton, Donald, & Smith, 1990; Lourdin, Della Valle, & Colonna, 1995; Liu & Scanlon, 2003; Babin, Della Valle, Dendievel, Lourdin, & Salvo, 2007), but in most of the cases, the recipes were similar without too many changes in the content of the major ingredient. The question is whether this relationship is still valid when the density of the foam is modified by the addition of fibers and whether the relation between density and stress at rupture can be improved by taking into account the mechanical properties of the dense matrix containing different levels of fibers.

In order to decouple the effect of the foam density from the effect of the dense matrix when fibers are added in the recipe, and also to know to which extent the dense matrix influences the global mechanical properties of the foam, a model of composite materials can be used. The mechanical properties of dense materials may be classified according to different behaviors. They may be ductile, i.e. elastic or fragile, i.e. less able to deform under stress. The fragile behavior characterizes brittle materials, such as dry extruded cereals. Their brittleness gives them their crispy properties. Upon moisture uptake, extruded cereals become less brittle, more resistant to fracture and ductile (Fontanet, Davidou, Dacremont, & Le Meste, 1997; Roudaut, Dacremont, & Le Meste, 1998). For both ductile and fragile materials, the addition of particles such as fibers, may either reinforce or decrease the mechanical properties. This can usually be observed on the Young modulus of the materials and reflected through the maximal stress, i.e. hardness. The reinforcing or fragilizing effects of the added fibers or particles depend on the way they interact with the continuous phase (Leclair & Favis, 1996). The model of Nicolais and Nicomedo (1974) describes the stress at rupture of a composite, $\sigma_c$, according to the volume fraction of particles, $V_P$: $\sigma_c = \sigma_M \cdot (1 - aV_P)^b$, where a is a constant linked to the adhesion between continuous phase and particles (fixed to 1.21 for low adhesion), $b$ is linked to the geometry of the particles (fixed to 2/3 for spherical particles) and $\sigma_M$ is the stress of the continuous phase. This model has been shown to fit the experimental data very well in previous studies dealing with extruded starch/zein blends (Chanvrier, Della Valle, & Lourdin, 2006; Habeych, Dekkers, van der Goot, & Boom, 2008).

The combination of both Gibson–Ashby relationship and Nicolais–Nicomedo model could be a way to decouple the impact of the different levels of structure; i.e. at the foam structure level and at the matrix (cell walls) level. This approach would be unique when starting from experimental data and would fill the gap regarding the impact of fibers. Previous studies reported in the literature mainly cover mechanical modeling of cereal solid food through finite element calculation (Liu & Scanlon, 2003; Guessasma, Babin, Della Valle, & Dendievel, 2008; Guessasma, Chaunier, & Lourdin, 2010; Guessasma, Chaunier, Della Valle, & Lourdin, 2011). In these studies, either products are composed of pure starch or only proteins are considered as particles. The present study will add more complexity in the recipes by taking into account the added fibers as particles on top of added proteins, starch still being the major component of the products.

The objective of this study was to enrich extruded cereals with soluble and non-soluble fibers, i.e. oat bran concentrate (OBC) and wheat bran, respectively. Two types of base recipe were explored: (i) a recipe mainly composed of wheat and (ii) a recipe mainly composed of corn and soya, the latter displaying a higher amount of proteins. For both recipe, starch is the main component. The properties of the extruded products were firstly assessed in terms of porous structure by X-ray tomography imaging followed by 3D image analysis and of mechanical properties through a compression test. In order to understand the impact of the fibers on the porous structure of the extrudates and also on their wall properties (i.e. intrinsic material properties), the Gibson–Ashby law was applied with normalization performed according to mechanical properties of composite materials. The behavior of composite solid foams was thus discussed by considering fibers and proteins as particles filling the main starchy phase of the extrudates. Finally, the impact of the fibers content and types on the two base recipes was also discussed with regards to the composite behavior of the walls in both recipes.

## 2. Materials and methods

### 2.1. Materials

Whole wheat flour type 550 (Provimi Kliba S.A., Switzerland), wheat bran (Provimi Kliba S.A., Switzerland), wheat flour (Groupe Minoteries S.A., Switzerland), oat bran concentrate (OBC) Crisp flat 18% (Rubinmuhle, Germany), corn semolina (Champagne maïs, France), whole toasted soya flour (Haefliger AG, Switzerland), sucrose (Zuckerfabriken Aarberg, Switzerland) were used as ingredients for the production of the extruded cereal products. Two types of recipes were produced: one mainly composed of whole wheat, refined wheat and corn flours (Exp1) and the other mainly composed of corn and soya flours (Exp2). The detailed product compositions are presented in Tables 1 and 2. All recipes contain 2% of sugar in the extruded base.

### 2.2. Production of cereal-based products by extrusion

The extrusion trials were conducted using a co-rotating twin-screw extruder (BC21 extruder, Clextral, Firminy, France) with a barrel length of 400 mm, a screw diameter of 25 mm, a length-to-diameter ratio of 16:1 and a die opening of 2.5 mm. The screw configuration was composed of conveying and mixing elements. The extruder was operated at a constant feed rate of 15 kg/h. The four heating zones of the barrel were kept at a temperature of 90 °C, 135 °C, 150 °C and 160 °C, respectively. The temperature of the product at the end of the extruder was 135 °C. The screw speed was set at 400 rpm.

For the production of Exp1 and Exp2 products, the ingredients were mixed prior to extrusion with a solid mixer (Prodima Ac-Li-50, Switzerland) and introduced into the extruder using a co-rotating twin screw K-Tron feeder (K-Tron Co, Niederlenz, Switzerland). Water at ambient temperature (20 ± 2 °C) was injected at a controlled rate with a syringe pump. It was adjusted during extrusion at 20% for Exp1 and 15.2% for Exp2.

After obtaining stable extrusion variables, samples were collected and dried down to 2.7 ± 0.4% and 2.4 ± 0.5% moisture in a forced air convection oven at 120 °C. Extruded products were then cooled down to room temperature. The specific weight of the uncoated extruded cereals was measured by weighing in duplicate the dry extrudates in a 500 mL cylinder. All samples were then prepared in uncoated and coated forms. The coating consisted of a syrup composed of sucrose (67%), dextrose (5%) and water (28%) (*TS* = 72%). The samples were coated with 29.4% w/w syrup. All samples were sealed in aluminum bags at ambient temperature (20 ± 2 °C) until evaluation. The moisture contents of the coated finished products are presented in Tables 1 and 2 for both Exp1 and Exp2.

### 2.3. Mechanical properties

Mechanical properties of extruded cereals were measured with a Texture Analyzer TA. HDI (from Stable Micro Systems) equipped with a 500 kg load cell. A 10-plate Kramer shear cell was used to

**Table 1**
Characteristics of the samples of Exp1 in terms of flours present in the recipe, carbohydrates and proteins content, matrix and particles content and porosity (WG: whole grain, OBC: oat bran concentrate, WB: wheat bran).

| Samples | Whole wheat (%) | Wheat flour (%) | Corn flour (%) | OBC (%) | WB (%) | Proteins (%) | Fibers (%) | Product moisture (%) | Carbohydrate (%) | Particles (%) | Porosity (%) |
|---|---|---|---|---|---|---|---|---|---|---|---|
| WG40 | 40 | 40 | 18 | 0 | 0 | 10 | 4.8 | 5.4 | 67.9 | 14.8 | 91.6 |
| WG40/OBC10 | 40 | 30 | 18 | 10 | 0 | 10.6 | 8.2 | 4.4 | 63.9 | 18.8 | 89.2 |
| WG40/WB10 | 40 | 30 | 18 | 0 | 10 | 10.4 | 8.4 | 5 | 63.5 | 18.8 | 88.2 |
| WG40/OBC20 | 40 | 20 | 18 | 20 | 0 | 11.2 | 11.6 | 2.5 | 59.8 | 22.8 | 86.8 |
| WG40/WB20 | 40 | 20 | 18 | 0 | 20 | 10.7 | 12 | 7.1/1.6 | 59.1 | 22.7 | 84.1 |
| WG60 | 60 | 20 | 18 | 0 | 0 | 10.1 | 6.2 | 4.2 | 65.9 | 16.3 | 89.6 |
| WG60/OBC10 | 60 | 10 | 18 | 10 | 0 | 10.7 | 9.6 | 5.5 | 61.9 | 20.3 | 88.5 |
| WG60/WB10 | 60 | 10 | 18 | 0 | 10 | 10.5 | 9.8 | 4.7 | 61.5 | 20.3 | 87.4 |
| WG60/OBC20 | 60 | 0 | 18 | 20 | 0 | 11.3 | 13 | 3.8 | 57.8 | 24.3 | 85.5 |
| WG60/WB20 | 60 | 0 | 18 | 0 | 20 | 10.9 | 13.4 | 2.0 | 57.1 | 24.3 | 84.9 |
| WG80 | 80 | 0 | 18 | 0 | 0 | 10.3 | 7.6 | 4.7 | 63.9 | 17.9 | 90.5 |
| WG80/OBC10 | 80 | 0 | 8 | 10 | 0 | 11.4 | 11 | 4.4 | 59.3 | 22.4 | 86.6 |
| WG80/WB10 | 80 | 0 | 8 | 0 | 10 | 11.1 | 11.2 | 5.6 | 58.9 | 22.3 | 86.6 |
| WG80/OBC20 | 80 | 0 | 0 | 18 | 0 | 12.2 | 13.7 | 7.2/1.7 | 55.5 | 25.9 | 83.3 |
| WG80/WB20 | 80 | 0 | 0 | 18 | 0 | 11.8 | 14.1 | 5.2 | 54.9 | 25.9 | 82.6 |

crush the extruded cereals placed as a 17 mm thick bed. The thickness of the sample bed was chosen to stand in the optimal range of measurement of the force (0.5% precision). The Kramer shear test was carried out on the coated finished extruded cereals. The crosshead speed was 1 mm/s across a displacement of 40 mm. Three replicates were performed for each sample.

From the force–displacement curves, different values were extracted: (i) $F_{max}$ (N), corresponding to the maximum of the curve, i.e. the maximum force or the breaking force and (ii) $N_{peak}$, the number of peaks obtained on the jagged curve above a force threshold of 1 N.

The rationale for using Kramer cell was to try and extract other attributes from the force–displacement curve (not presented in this manuscript). On Exp1, compression test with a flat probe was also performed (circular plate of 50 mm). $F_{max}$ with flat probe was linearly correlated to $F_{max}$ with Kramer cell. Even though the bed of cereals is fully crossed by the Kramer cell, $F_{max}$ follows same trend for both types of measurements applying more or less shear. The volume of cereals bed is kept constant (8.2 cm × 6.5 cm × 2 cm). The bed is composed of extruded balls and is itself a solid foam, with air in the balls and between the balls. All products are in the same range of size; the air voids between balls can be assumed to be identical. Consequently, for maximal stress calculation, $F_{max}$ was divided by the total surface of Kramer cell, i.e. 10 pieces with a contact surface of 3 × 70 mm$^2$. The surface is then 21 cm$^2$.

### 2.4. Structure of extruded cereals assessed by X-ray tomography

X-ray tomography scans were acquired with a 1172 MCT system (Brüker MicroCT, Kontich, Belgium) with a X-ray source of 40 kV and 100 μA. For a pixel size of 5 μm, the camera was set up at 2000 × 2096 pixels with an exposure time of 295 ms. Scans were performed on a representative specimen of each experiment over 180°, the rotation step was 0.4° and the frame averaging was 10. The reconstruction of datasets was performed on average over 450 slices with Brüker MicroCT recon software (version 1.4.4.).

3D image analysis was performed on 10 μm per pixel datasets with CTAn software (version 1.7.0.3, 64 bit, Brüker MicroCT, Kontich, Belgium). After segmentation of the grey level images at 40, the selection of the volume of interest was performed through the shrink-wrap function to adjust to the surface or contour line of extruded pellets. The porosity of the pellets was then calculated as the ratio of the volume of pores to the extrudate volume, the extrudate volume being equal to the volume of interest previously defined. The relative density corresponds to the ratio of volume of materials to the volume of extrudate. The structure separation function gave the cells size distribution and the thickness separation function gave the walls thickness distribution, and their mean values calculated from the distribution in volume.

## 3. Results

### 3.1. Structure of extruded cereals assessed by X-ray tomography

Fig. 1 presents representative cross-sectional X-ray tomography images of the extruded products of Exp1. The visual observation shows that regardless of the amount of added fibers in the recipe, increasing the amount of whole grain (WG) flour induces more compacted products (with smaller diameter of the products). The cells look also globally smaller. For a fixed amount of WG in the recipe (40%, 60% or 80%), increasing the added fibers content, regardless of the types of fibers, also induces a loss of expansion and a decrease of cell size. The most compacted product is obtained for the highest amount of WG and 20% wheat bran (WB).

**Table 2**
Characteristics of the samples of Exp2 in terms of flours present in the recipe, carbohydrates and proteins content, matrix and particles content and porosity (CF: corn flour, OBC: oat bran concentrate, WB: wheat bran).

| Samples | Corn flour (%) | Soya flour (%) | OBC (%) | WB (%) | Proteins (%) | Fibers (%) | Product moisture (%) | Carbohydrate (%) | Particles (%) | Porosity (%) |
|---|---|---|---|---|---|---|---|---|---|---|
| CF64 | 64 | 34 | 0 | 0 | 17.4 | 5.4 | 3.6 | 55.6 | 22.8 | 90.0 |
| CF50/OBC14 | 50 | 34 | 14 | 0 | 19.0 | 10.1 | 2.8 | 49.0 | 29.1 | 85.9 |
| CF50/WB14 | 50 | 34 | 0 | 14 | 18.6 | 10.4 | 2.2 | 49.5 | 29.0 | 76.8 |
| CF44/OBC20 | 44 | 34 | 20 | 0 | 19.6 | 12.2 | 3.1 | 46.2 | 31.8 | 75.6 |
| CF44/WB20 | 44 | 34 | 0 | 20 | 19.1 | 12.6 | 2.7 | 45.5 | 31.7 | 76.8 |
| CF38/OBC26 | 38 | 34 | 26 | 0 | 20.2 | 14.2 | 3.7 | 43.4 | 34.4 | 62.9 |
| CF38/WB26 | 38 | 34 | 0 | 26 | 19.7 | 14.8 | 2.5 | 42.5 | 34.5 | 74.8 |
| CF32/OBC32 | 32 | 34 | 32 | 0 | 20.9 | 16.2 | 1.5 | 40.6 | 37.1 | 59.2 |
| CF32/WB32 | 32 | 34 | 0 | 32 | 20.2 | 16.9 | 3.2 | 39.5 | 37.1 | 73.3 |

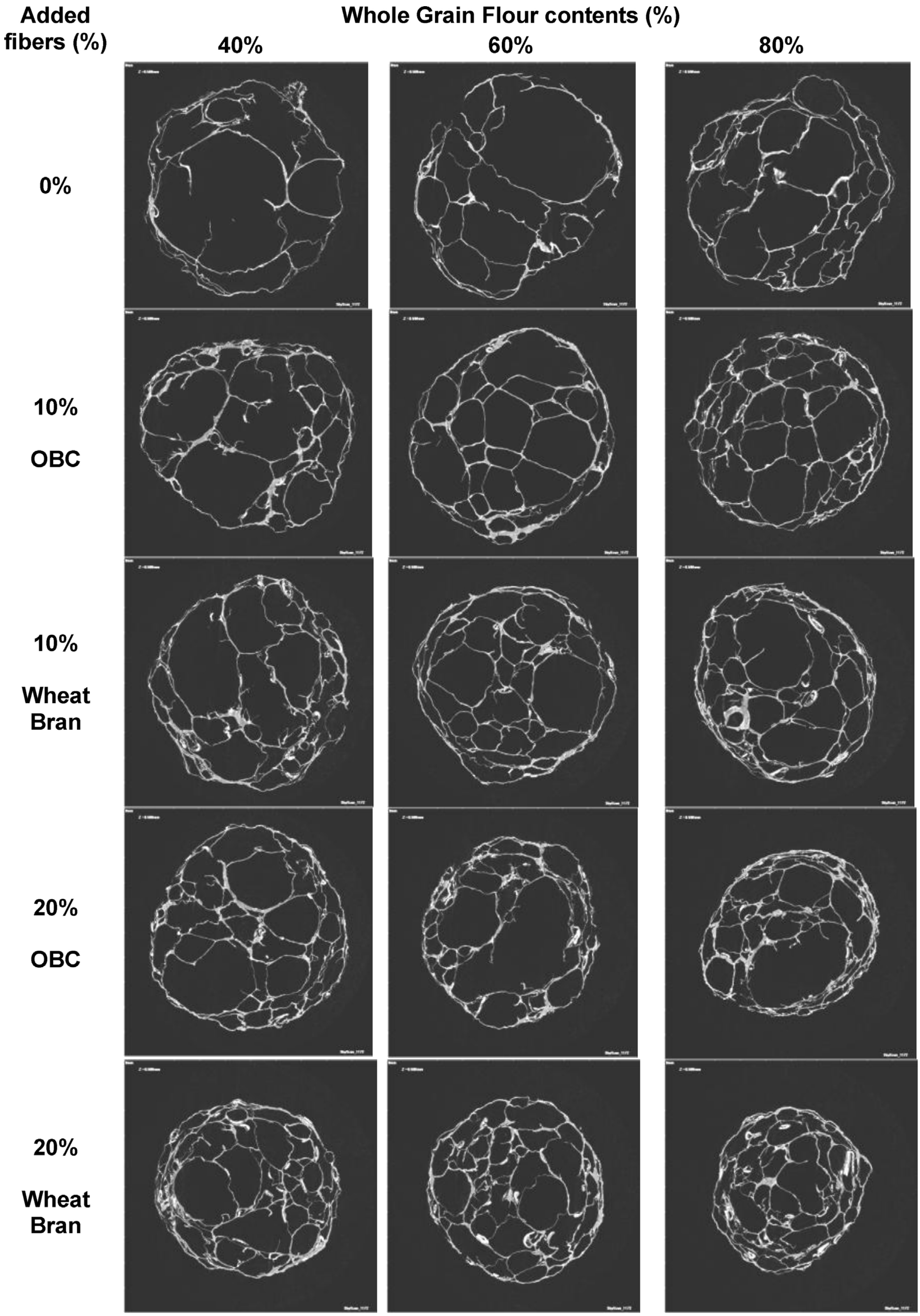


**Fig. 1.** Representative cross-sectional X-ray tomography images of the extrudates of Exp1 (OBC: oat bran concentrate).

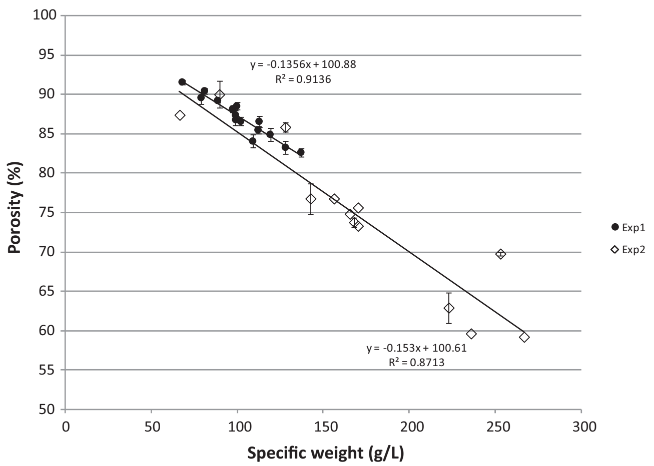


**Fig. 2.** Porosity (%) obtained by 3D image analysis of X-ray tomography images versus specific weight (g/L) of the extruded products for Exp1 and Exp2.

The most aerated product is the one with 40% WG and no added fibers. These observations are not unexpected and consistent with the results reported in the literature concerning fibers addition in extruded cereals (Brennan et al., 2008; Yao, Jannink, Alavi, & White, 2006). However, in this study, the 3D image analysis performed on the X-ray tomography images gave more insight on the expanded structure than destructive microscopic 2D observations.

Since the observation of the X-ray tomography images only gives a visual impression of the structure, a quantification of this structure has been performed through 3D image analysis in order to get an objective comparison of the different extrudates.

Fig. 2 shows a linear negative correlation between the porosity of the extrudates assessed by 3D image analysis and the specific weight. This correlation is valid for both experimental designs. The method developed for 3D image analysis on the X-ray tomography images is thus validated by the physical measurement of the specific weight.

The structural attributes such as porosity and mean cells size (MCS) of the extrudates were plotted against the total dietary fibers content (TDF) of each product (Fig. 3a and b). Both porosity and MCS decrease when TDF increases, thus showing the strong impact of the fibers levels in the recipe on the foam structure of the extrudate. If the trends are similar for Exp1 and Exp2, for the latter, the TDF increase induces a higher loss of porosity. This result may be explained by two reasons: (i) the difference of granulometry of the fibers used for Exp1 and Exp2 (Carvalho, Takeiti, Onwulata, & Pordesimo, 2010). Due to segregation between fibers and the other components of the recipe in Exp2 during dry mixing, the particles size of the fiber has been reduced through milling. This segregation did not happen for Exp1, the fibers were thus used as such and had larger particles size. It is assumed that this segregation was due to the presence of soya in Exp2. The presence of soya flour certainly creates larger range of specific weights within the flours of the recipe.

The milling of the fibers for Exp2 increases the specific surface between the fibers and the matrix, thus possibly changing the amount of interactions between fibers, starch and proteins during the expansion step. Moreover, products from Exp2 contain a higher amount of proteins due to the presence of soya flour: Protein content stands between 10% and 12% for Exp1 whereas it stands between 15% and 23% for Exp2. This higher amount of proteins in Exp2 may also modify the amount of interactions between the starch/protein matrix and the fibers in comparison to Exp1, which displays a preponderant starchy matrix (Table 1).

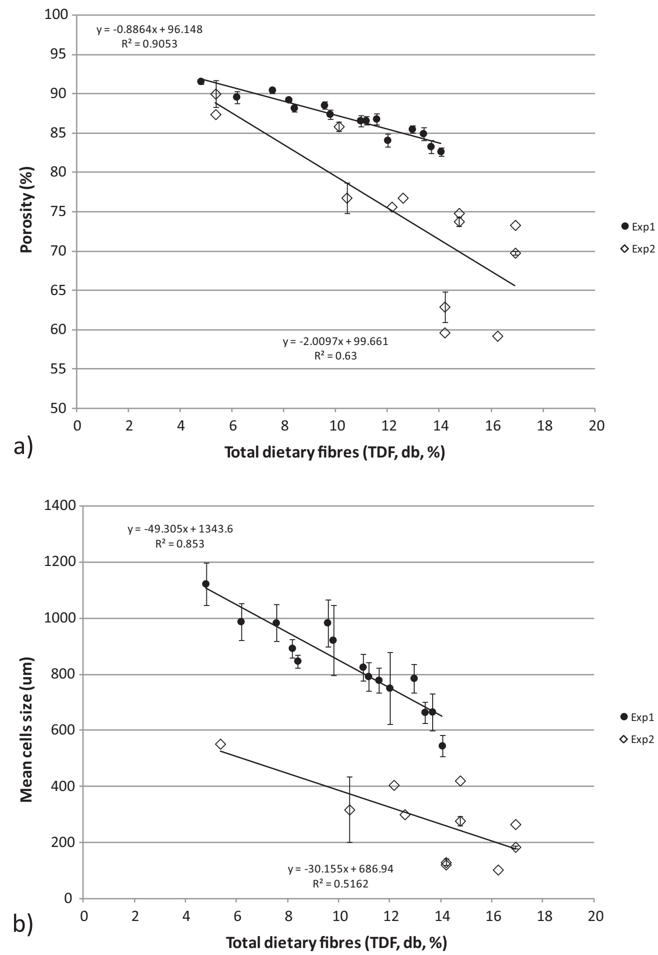


**Fig. 3.** Structural attributes of extruded cereals versus total dietary fibers content (%): (a) porosity (%) and (b) mean cells size (μm).

For both experimental designs, the loss of porosity with TDF is linked to smaller cells (Fig. 3b). This is certainly due to the limitation of the expansion of the cells at the end of the die due to the presence of fibers. Some hypotheses have already been developed to explain this phenomenon (Robin et al., 2011a), such as cell breakage during expansion at the interface between starch and fibers, thus decreasing the driving pressure for cell growth (Chanvrier et al., 2007) and also loss of elasticity of the melt as measured by on-line capillary rheometry (Robin et al., 2012). If the trends are similar for both experimental designs, the absolute values are different; cells are smaller in Exp2 than in Exp1 (Fig. 3b). This is certainly due to the higher amount of proteins in Exp2 which may change the elastic properties of the melt (Chanvrier et al., 2006) and limit the stretching of the walls during expansion at the end of the die when the product is still in the rubbery state. This is in accordance with the observations of Yu, Ramaswamy, and Boye (2013), who reported a loss of expansion when extruding soya proteins–corn flour blends with increased levels of soya.

The combination of high levels of proteins with increased TDF is detrimental for the expansion of the extrudates. It is either a matter of rheological properties of the products in this state which may be less stretchable with possibly less elasticity, higher shear viscosity or even elongational viscosity and/or a matter of morphology of the walls that may rigidify the products under expansion (Xanthos, 2005; Pai, Blake, Hamaker, & Campanella, 2009).

### 3.2. Mechanical properties of the extruded cereals

The main impact on the maximum force is porosity. Maximum force, $F_{max}$, measured during a compression test of the extrudates, represents the hardness of the products and is usually linked to the sensory hardness perception (Roudaut, Dacremont, Vallès Pamies, Colas, & Le Meste, 2002). $F_{max}$ decreases when porosity increases, regardless of the fiber type and the base recipe (Fig. 4a). This trend is observed for both Exp1 and Exp2, however, the absolute values of hardness ($F_{max}$) stand above for some samples of Exp1. For similar porosity, the trend shows that Exp1 would have higher hardness. Two explanations are possible for this observation: (i) the difference of composition of the walls with higher levels of proteins for Exp2, (ii) the moisture content of the extrudate; the average moisture levels for Exp1 is 4.7% whereas it is 3.1% for Exp2. Products with higher moisture content (Exp1) may be more elastic and less brittle thus leading to higher $F_{max}$. However, not too many conclusions should be drawn from this observation since in the range of 85–90% porosity, products from both experimental designs display similar values of $F_{max}$, and there is no product of Exp1 in the range of 60–80% porosity. Moreover, two variants of Exp1 have a much higher moisture level (7%) which may induce a bias in the trend. This issue will be addressed in the next part with the application of the Gibson–Ashby law for cellular foams.

Fig. 4b displays the number of peaks extracted from the force–displacement plot of the compression test. In previous works in the case of puncture test, some authors described the NSR (number of spatial ruptures) as the ratio of the total number of peaks to the distance of puncturing and found a correlation with crispness of products, as determined by sensory analysis (Valles Pamies, Roudaut, Dacremont, Le Meste, & Mitchell, 2000; Roudaut et al., 2002). In our study, where a compression test was used, the number of peaks reflects the number of fractures events occurring in the products upon compression and breakage. $N_{peak}$, which can also be an attribute reflecting crispness, tends to increase when porosity increases. In the range of 80–85% porosity, Exp1 displays fewer peaks than Exp2. This may be explained by the same reasons mentioned above, i.e. lower amount of proteins in Exp1 thus inducing a different morphology of the walls and possibly a difference in the fracture mechanisms, and/or moisture discrepancies between the experimental designs. The fracture event occurring in the walls reflects the cracks propagation within the solid cereal

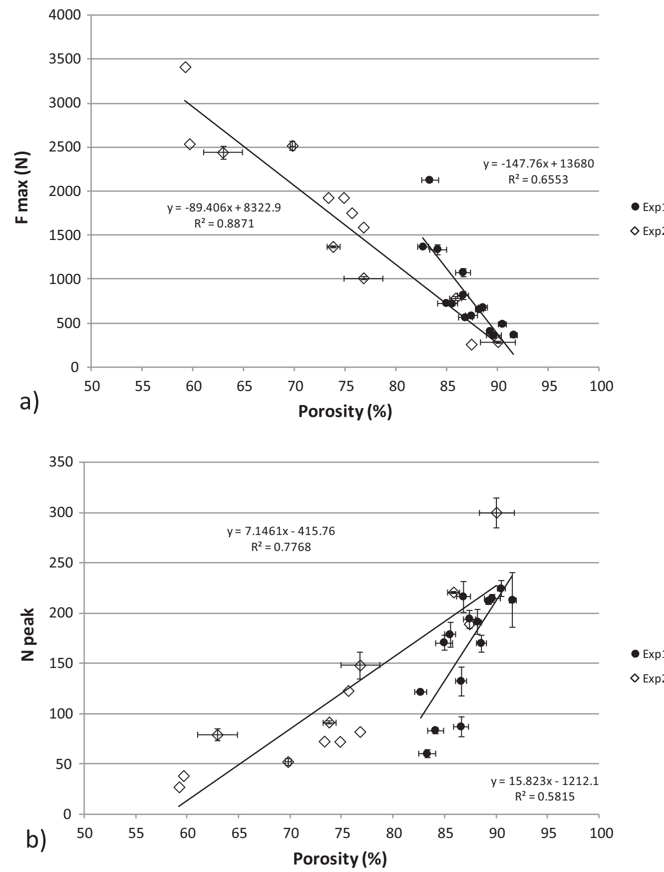


**Fig. 4.** Mechanical properties of the extruded cereals from Exp 1 and Exp2 obtained by compression test with Kramer cell: (a) maximum force, $F_{max}$ (N) and (b) peak number, $N_{peak}$ versus Porosity (%).

foams, as studied by Hedjazi, Guessasma, Della Valle, & Benseddiq (2011). The crack propagation is driven by the concentration of local stresses and is certainly dependent on both lengthscales of structure: expanded structure and walls morphology, as suggested by our present results.

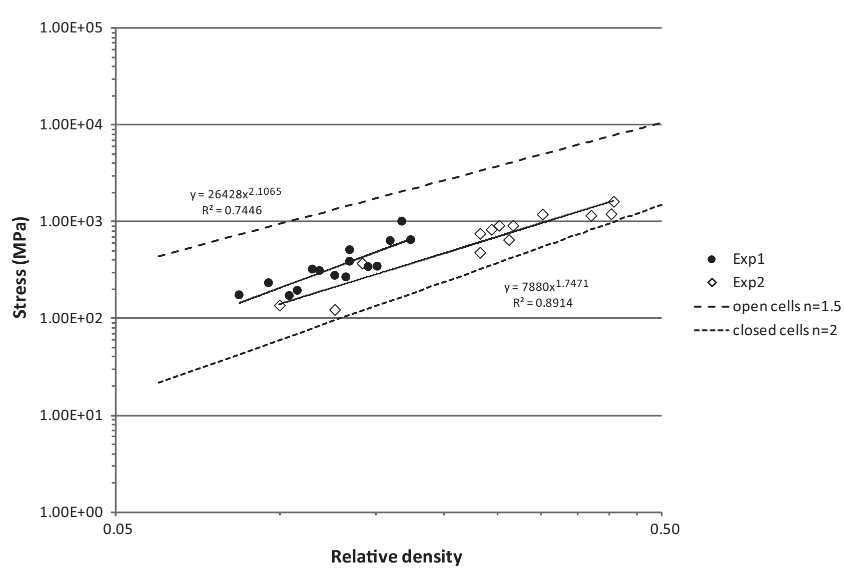


**Fig. 5.** Maximum stress (stress max.) versus relative density of extruded cereals for Exp1 and Exp2 in comparison to Gibson–Ashby law for open and closed cells.

**Table 3**
Correlation coefficients $R^2$ of the Gibson–Ashby fit for the different corrections and normalization applied (OBC: oat bran concentrate, WB: wheat bran).

| | Exp1 | Exp2 | Exp1–Exp2 | Exp1–Exp2 without two outliers | Exp1–Exp2 with corrections for two outliers |
|---|---|---|---|---|---|
| No normalization | 0.745 | 0.891 | 0.802 | 0.901 | 0.880 |
| | | | $V_p$ = fibers | | |
| All fibers | 0.796 | 0.886 | 0.804 | 0.899 | N.C. |
| OBC | 0.774 | 0.918 | N.C. | N.C. | N.C. |
| WB | 0.875 | 0.929 | N.C. | N.C. | N.C. |
| | | | $V_p$ = fibers + proteins | | |
| All fibers | 0.798 | 0.886 | 0.862 | 0.927 | 0.914 |
| OBC | 0.779 | 0.919 | 0.853 | N.C. | N.C. |
| WB | 0.877 | 0.928 | 0.878 | N.C. | N.C. |
| | | $V_p$ = fibers + proteins and normalization with walls thickness | | | |
| All fibers | N.C. | N.C. | 0.905 | 0.937 | 0.931 |

N.C. Not calculated.

## 4. Discussion

### 4.1. Application of the Gibson–Ashby relationship

In this part, relative density is considered instead of porosity. Relative density is easily calculated from porosity as described in the X-ray tomography method. The range of relative density obtained (from 0.08 to 0.17 for Exp1 and from 0.09 to 0.40 for Exp2) allows applying the Gibson–Ashby relationships for cellular solids.

#### 4.1.1. Gibson–Ashby relationship for Exp1 and Exp2

The Gibson–Ashby model has been applied for both Exp1 and Exp2 separately and plots of stress versus relative density are presented in Fig. 5. Stress corresponds to the maximal stress calculated from the $F_{\max}$ values obtained for the extrudates and presented above in the results chapter. Even though the maximum stress of the dense materials, i.e. the constitutive materials of the walls of the extrudates, has not been considered yet, the correlation coefficients are already good (Table 3, $R^2$ of 0.745 for Exp1 and 0.891 for Exp2). This representation shows in a clearer manner that Exp1 displays higher values of stress than Exp2. The reasons for this result were already discussed in the previous part (difference in moisture and/or proteins levels). The exponent obtained for Exp1 is close to 2, thus reflecting a structure which certainly has closed cells. For Exp2, the exponent is 1.75. For both recipes, same trends are observed versus relative density, but the absolute values are different.

When combining the data of Exp1 and Exp2 and applying the Gibson–Ashby equation, the correlation coefficient $R^2$ is 0.802. This value is rather good as well, thus showing that mechanical properties of the extrudates of both experimental designs are mainly dominated by their relative density. Indeed, in this case, the mechanical properties of the intrinsic materials of the walls are not taken into account in the equation.

#### 4.1.2. Application of the model of Nicolais and Nicomedo

The improvement of the fit of the Gibson–Ashby relationship can be undertaken by including the maximum stress of the intrinsic materials. Since it would have been extremely difficult and time-consuming to produce dense materials with the same composition of the expanded extrudates and to characterize them mechanically, the following approach has been used. It was shown earlier in past studies that dense extruded corn cereals could be considered as matrix/particles materials with regards to their morphology and their mechanical properties: the matrix being the starchy phase, the particles being the proteins and the adhesion being low between them (Chanvrier et al., 2006; Habeych et al., 2008). For starch-based extruded cereals enriched in fibers, the matrix can also be the starchy phase and the particles (or dispersed phase) can be assumed to be the proteins and the fibers (Robin et al., 2011b). Even though the proteins content is up to 23% in some recipes, they can still be considered as particles and not as matrix. Indeed, the percolation threshold of the proteins, i.e. the amount of proteins at which the inversion phase takes place, was measured between 19% and 38% of proteins for starch/protein blends (Chanvrier et al., 2006). Since 23% stands at the lower limit of the co-continuity morphology, in our products proteins are either fully dispersed or dispersed with a slight co-continuity with starch, but they definitely are not fully continuous. Low adhesion between those components is also assumed. Consequently, the model of Nicolais and Nicomedo (1974) can be applied.

In this purpose, the value of the maximum stress of a dense material of pure non-granular starch was obtained from the literature (Nicholls, Appelqvist, Davies, Ingman, & Lillford, 1995; Guessasma et al., 2011). The value of 100 MPa was used in this study as an average of values obtained by bending test. Of course, same solicitation mode, i.e. compression, as the extruded balls cannot be achieved on dense materials. Using values obtained from bending is acceptable since bending of the cereals walls occurs during their compression with Kramer cell. In bending, tensile and compression occur in the materials. The fibers and proteins content expressed as a percentage of the recipe (w/w) were converted into volume fraction of the recipe, as required in the Nicolais–Nicomedo equation (Nicolais and Nicomedo, 1974). The use of this equation always induces a maximum stress of the composite lower than the one of the matrix alone. Indeed, due to the low adhesion hypothesis, the volume fraction of particles or fillers is considered to act as a fragilizer for the starch matrix. The higher the volume fraction of particles, the lower the maximum stress, thus meaning that the material is less resistant. The decrease of maximal stress is dependent on the strength of interaction between the filler and the matrix, i.e. for cereals, the type of proteins (Zeng et al., 2011).

#### 4.1.3. Data normalization including fibers and proteins as particles

The Gibson–Ashby relationship including the calculated maximal stress of the dense starchy materials was applied for different configurations: (i) including the volume fraction of fibers only and (ii) including the volume fraction of both fibers and proteins. The first configuration does not improve much the fit when combining the data of both Exp1 and Exp2 (Table 3). However, when considering the volume fractions of both fibers and proteins, the fit is significantly improved ($R^2$ increases from 0.804 to 0.862). Basically, including protein effects allowed building a master curve including data of both Exp1 and Exp2. This normalization of the data allowed eliminating or reducing the discrepancies due to different protein contents in the recipes. The range of proteins content was larger for Exp2 than for Exp1, as described in Section 2.1.

The negligible improvement through the fibers normalization can thus be explained by the fact that the ranges of TDF are very close between Exp1 and Exp2 (between 5% and 16% for both). In conclusion, after normalization for fibers and proteins impact on the dense materials, both recipes not only show similar behaviors in terms of maximal stress versus relative density, but are also aligned regarding the absolute values of maximal stress.

The discrepancies towards the Gibson–Ashby equation ($R^2$ = 0.862) and to the perfect fit can be attributed to the elements that are neglected in both the Gibson–Ashby fit and the Nicolais–Nicomedo model. First of all, at the level of the porous structure, only the impact of the relative density is considered. But the cells size distributions and the walls thickness distribution could have an impact as well. The way cells and walls size are distributed in the products may indeed impact the fracture behavior of the whole structure. The foam structure of the extruded cereals displays a lot of irregularities that may move the breaking behavior away from the Gibson–Ashby relationship. Secondly, at the scale of the biopolymers phase, the dispersed particles are considered as spherical and homogeneously dispersed. However, in reality, proteins and fibers particles have different size and are randomly spread in the starchy matrix. The shape of the particles is not obviously spherical: Elongated shape for fibers and possible packed protein aggregates for proteins. In material science, the packing arrangement of particles is known to impact the mechanical properties of the material (Kastner, Kickinger, & Salaberger, 2011; Mazzola, Bemporad, Squeo, Trovalusci, & Tagliaferri, 2011). Finally, it could even be that for the highest protein level, some fibers are locally embedded in a protein matrix, itself dispersed in the starchy phase. The quality of the contact between the starchy matrix and the particles, i.e. fibers or proteins, supposed to be of low adhesion, may be modified according to the surface contact and the type of contact between components: starch/proteins, starch/fibers, fibers/proteins.

Neither the quality of these contacts nor the surface contacts were possible to assess. The surface contacts determination would require microscopic observations with specific staining complemented with image analysis for quantification, but has not been undertaken in this study due to the complexity of the recipes.

When the data are fitted separately for OBC and WB, the correlation coefficient is improved for WB products and decreased for OBC. This result may reflect some of the above-mentioned causes of discrepancies: difference of shapes between OBC and WB, difference of size, difference of adhesion between starch/WB and starch/OBC and possibly, different molecular changes of WB and OBC upon processing (Tosh et al., 2010).

In a previous work considering expanded extruded flat breads composed of different ratios of amylose and amylopectin (Babin et al., 2007), the $R^2$ of the Gibson–Ashby fit is rather low (0.51). The scattering of the data was mainly related to the cellular structure of the foam: The more dispersed the cell wall size distribution, the less resistant the foam. In order to improve the fit, the walls of these products could also be considered as composites of amylose and amylopectin. Due to steric effects, these two macromolecules are incompatible and one may be dispersed in the other, with regards to their respective content. Applying the Nicolais–Nicomedo equation similarly to our study could confirm or infirm the composite behavior of the walls. Indeed, in this case, the behavior of the walls may be at the edge between composite-type behavior (particles dispersed in a matrix) and biopolymer blends (e.g. macromolecules blended together with domains enriched in amylose dispersed in a continuous phase of amylopectin). In extruded products, proteins can be considered as particles because they form compacted aggregates as observed by microscopy (Chanvrier et al., 2006). The proteins aggregation also occurs during the extrusion process at the molecular level with formation of disulfides bonds (Fisher, 2004).

*4.1.4. Data normalization with walls thickness*

In a second step, the thicknesses of the walls of the cells were also included in the normalization. Indeed, during compression of the extrudates, the breaking behavior of the walls is not only dependent on their composite properties, but also on their thickness. The ability to break off a cell wall is also obviously governed by its thickness, as mentioned by Babin et al. (2007): The more dispersed the walls size, the less resistant the foam. Consequently, including the walls thickness in the correction may also be a way to consider the heterogeneity of the foam structure. Since the walls size distributions cannot be used as such for the normalization, the data were normalized with the means walls thickness values. The Gibson–Ashby fit was improved from 0.862 to 0.905 for the correlation coefficient (Table 3), thus showing the relevance of the walls thickness effect on the mechanical properties of the foam.

An improvement of the fit was obtained along the whole process of normalization by fibers, protein contents and walls thickness. This allowed building a master curve independent of the base recipe of the extruded cereals. These normalizations are valid for cereals in the case of recipes where starch is the main component.

*4.1.5. Moisture correction for two outliers*

One of the important attributes of the product that impacts the mechanical properties of extruded cereals and that has not been discussed yet in this study, is the moisture content of the products. This subject will be thoroughly addressed in this paragraph.

All the products of each experimental design were extruded at the same level of moisture in the extruder. However, due to the difference of recipes and fibers content, it was difficult to obtain exactly the same level of moisture in the finished products, especially knowing that the capacity of fibers to bind water is higher than for starch. The majority of products displayed moisture contents between 2% and 5%, the average moisture level being 3.9%. In this range, we can assume that the moisture differences do not significantly impact the mechanical properties since the products are very dry and, at room temperature, very much below their glass transition temperature (Bizot et al., 1997). Moreover, previous studies show that significant changes in texture with increased moisture levels occur above 5% (Sauvageot & Blond, 1991; Fontanet et al., 1997; Roudaut et al., 1998). Nevertheless, two outlier products had higher moisture level of 7% and this value is critical since it stands above the threshold at which texture properties change considerably.

In order to check the impact of the two outliers on the Gibson–Ashby fit, they have been removed from the fit and the correlation coefficient increased from 0.905 to 0.937 (Table 3). This clearly shows that the two outliers had a strong impact and that moisture level definitely has to be uniform enough amongst samples to compare their mechanical properties. A higher moisture level can lead to an increase in elasticity of the material which may increase the maximal compression stress due to the higher ability of the material to deform. In order not to fully exclude them out of the study, the two outlier products were dried and then assessed again in terms of maximal compression stress. The drying led to moisture levels of 1.6–1.7%, which is lower than the average moisture contents of the products. In order to decrease possible bias, a corrected maximal compression stress was calculated at 3.9% moisture for both outliers. The calculation was performed proportionally to the stress values obtained at 7% and 1.6% moisture content. The data are plotted in Fig. 6. After all normalization and moisture correction, the correlation coefficient reached 0.931, which is quite high considering the difficulties of performing mechanical testing on heterogeneous and moisture-sensitive materials such as food. The global improvement of the correlation coefficient including normalization and moisture correction for two outliers went finally from 0.802 to 0.931.

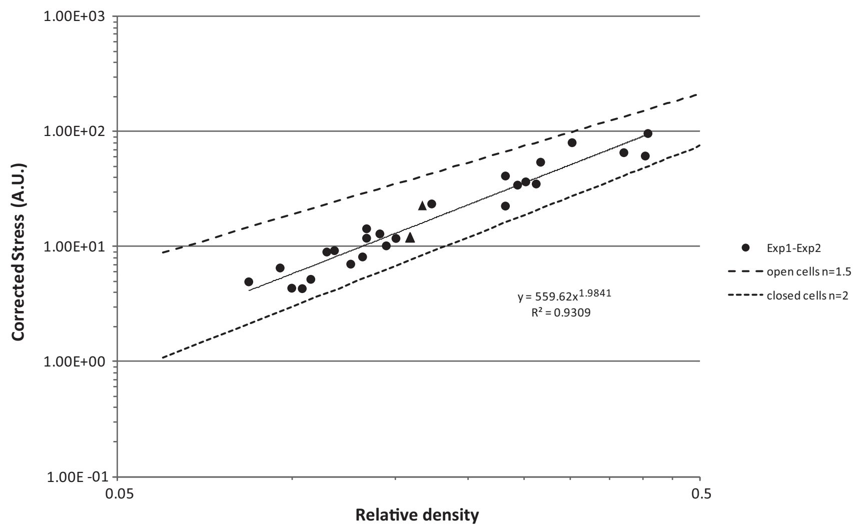


**Fig. 6.** Corrected stress versus relative density of extruded cereals for Exp1 and Exp2 together, in comparison to Gibson–Ashby law for open and closed cells. Round markers indicate cereals for which Stress Max. has been divided by the estimated stress max. of the dense materials (taking into account fibers and proteins content) and has been corrected by MWT. Triangular markers indicate the two outliers for which Stress Max. has been corrected for lower MC% (on top of the corrections described above for the other samples).

#### 4.1.6. *A foam structure with closed cells*

Fig. 6 shows the fit for which the exponent of the Gibson–Ashby is 1.96, very close to 2. This means that the cells are mainly closed and the structure is not open. Due to limit of resolution or contrast by X-ray tomography, it is difficult to define clearly by 3D image analysis whether a wall is completely closed or slightly open. According to the Ashby description of open cells, which look more like edges or thin bridges between cells, the cells of the extruded cereals are closed as visually observed on the X-ray images. The walls may be slightly discontinuous in some area thus giving narrow openings between cells but globally they exist in the products. A quick check has been performed with the Avizo software (Avizo 7.0, VSG3D, Bordeaux—partner of InsideFood project) allowing 3D characterization and image analysis of the X-ray tomography dataset. After the segmentation step, a dilatation was performed in order to remove the narrow openings within the walls. The further labeling of the cells of the cereals clearly indicated a good separation of the cells, observed visually in a 3D representation with different colors through a volume rendering. Further investigations can be undertaken with this software thanks to the labeling in order to gain more information on the cells characteristics themselves, such as shape information, circularity, etc.

### 4.2. *Impact of fiber types and of base recipe composition on the mechanical properties of the extruded cereals*

In order to observe the effects of the type of fibers and of the base recipe on the mechanical properties, maximal stress is presented in Fig. 7a and b for Exp1 and Exp2, respectively. Non-normalized data are used in this case; the normalization was performed in order to build hypothesis on the effects of other attributes than relative density on mechanical stress and the normalized data have shown that the Gibson–Ashby fit was improved. Consequently, the normalized data are only explained by the relative density, and the other effects of attributes tested, such as fiber types and content, proteins content and walls thickness, are not apparent anymore. Conversely, the corrected data for moisture level for the two outliers was used for this comparison.

### 4.3. *Focus on Exp2*

For Exp2, at 14% added fibers, there is a similar matrix–particles ratio between OBC and WB (49% starch and 29% particles, Table 2). The porosity is smaller for WB14 which explains its higher maximal stress than for OBC14, based on the Gibson–Ashby relationship. At 20% added fibers, again, WB20 and OBC20 display similar matrix and particles contents of about 46% and 32%, respectively. In this case, both products have a porosity of about 76%. This explains why their maximal stress is very similar (Fig. 7b). At 26% and 32% added fibers, the observation is similar: The matrix–particle content does not depend on the type of added fibers. However, in this case, porosity is lower for OBC than for WB, which leads to a higher maximal stress for OBC. This is the reverse when compared to 14% added fibers.

A question remains: Where does this inversion of trends for porosity with the increase added fibers come from? The most probable hypothesis suggests the limitation of expansion at the end of the die for high levels of OBC (above 26%). This limitation may be due to a change of OBC dispersion in the starchy matrix for high levels of OBC, which would induce a change in the elongational viscosity of the walls. Some studies have shown a strain hardening behavior of some biodegradable polymer blends depending on their composition (Eslami & Kamal, 2012).

### 4.4. *Focus on Exp1*

Based on the Gibson–Ashby fit and the matrix–particles interpretation, the very similar maximal stress obtained for WG40, WG60 and WG80 (without added fibers) can be explained by their very similar porosities (between 89.6% and 91.6%) and their very close starchy matrix–dispersed particles ratio (about 65% matrix, 16% particles; dispersed particles being fibers and proteins, Table 1). The slightly significantly higher stress obtained for WG80 may be explained by the difference of fiber contents (7.6% versus 6.2% and 4.8% of fibers, with proteins contents being very similar). This suggests a difference of adhesion or behavior of fibers versus proteins when dispersed in starch (due to differences of shape or behavior).

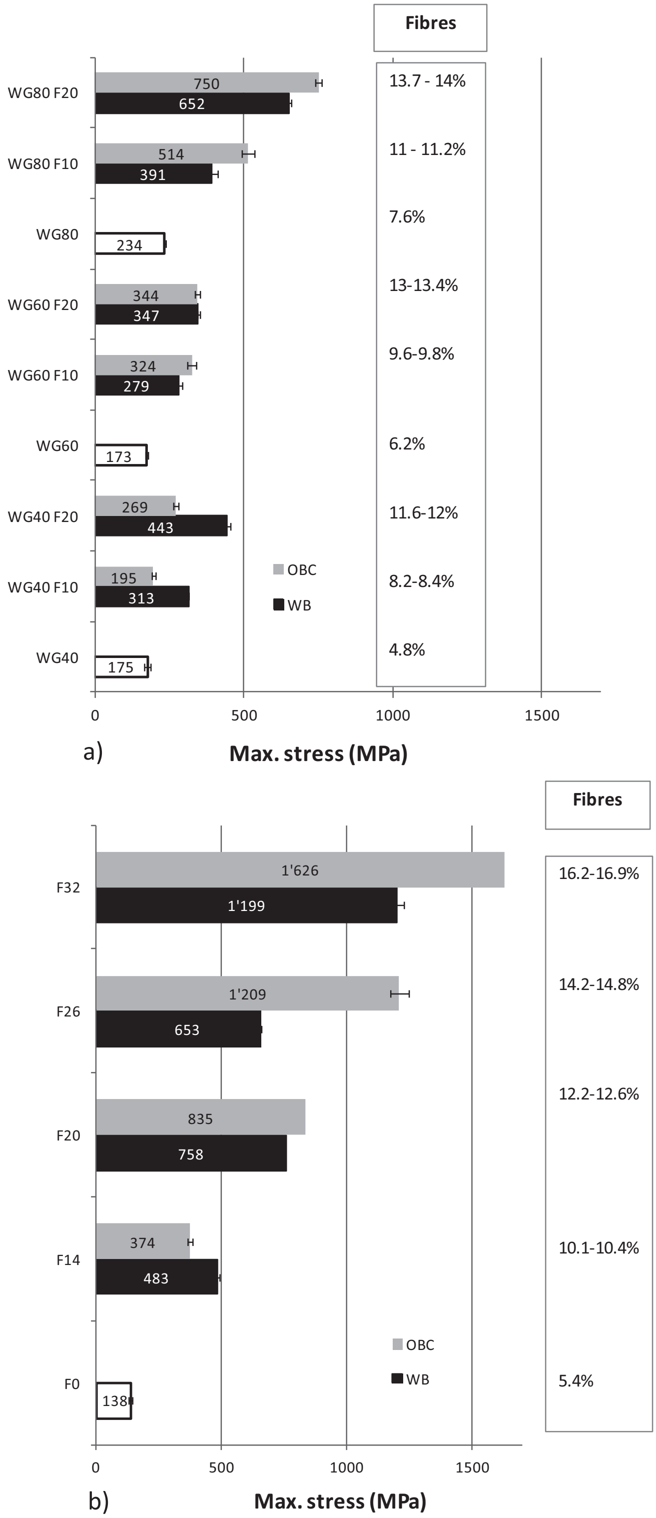


**Fig. 7.** Max. Stress (MPa) versus fibers types and content for both Exp1 (a) and Exp2 (b) (In Exp1 the outliers values due to high moisture levels have been corrected) (WG: whole grain, F: fibers, OBC: oat bran concentrate, WB: wheat bran).

For WG40 F10, the porosities and the ratio matrix–particles are similar for both OBC and WB products. However, the maximal stress is higher for WB (Table 1, Fig. 7a).

For WG80 F10, the same observation is made as for WG40 F10, i.e. the porosities and the ratio matrix–particles are similar. However, in this case, the reverse is observed; the maximal stress is higher for OBC. This peculiar behavior is consistent with the following hypothesis: At a specific threshold of particles concentration (and specifically fibers), some areas may become co-continuous with the starch phase. Similar behavior has been reported for starch matrices containing between 19% and 38% proteins (Chanvrier et al., 2006). In the present study, when getting closer to 25% particles, co-continuity may appear. Since WB is insoluble and OBC soluble, the co-continuity with starch may be reached at a different threshold concentration of WB and OBC, due to the difference of compatibility or miscibility with starch (Ajji and Utracki, 2002; Avérous & Boquillon, 2004; Avérous, 2004). A better miscibility combined with a co-continuous morphology for OBC would reinforce the mechanical properties of the cell walls of OBC, versus WB. These observations and hypothesis are also valid for F20 products.

For WG 40 and WG 60 (for F10 and F20), maximal stresses are respectively lower for OBC or not significantly different. This may be attributed to different particles size distribution of the added fibers, different shape of fibers, and different dispersion of the fibers in the continuous phase. However, at this stage, we cannot conclude. Only microscopic observations of the walls with stained particles (e.g. confocal scanning light microscopy) would help identifying the right hypothesis.

In summary, since the switch of trend occurs at WG60 with an increasing dispersed phase content, where the matrix represents 60% of the materials and the dispersed phase represents 20%, we may assume that it is linked to the morphology of the dispersed phase in the matrix. This morphology is known to be affected by the shape of the particles, the compatibility between phases (Utracki, 2002), the granulometry and the percolation threshold. All these characteristics are certainly different between OBC and WB.

This hypothesis of different spatial distributions of fibers according to the type of fibers is coherent with the hypothesis developed for Exp2. Nevertheless, for Exp1, due to less protein in the recipes, the expansion at the end of the die is not impacted. Similar porosities are obtained for OBC versus WB. The preponderant effect is thus the hardness of the walls. The latter is impacted by a possible lower percolation threshold for OBC than for WB.

#### 4.4.1. Importance of the spatial dispersion of particles

Finally, in Exp1, for same fibers content, there is a negligible impact of fibers type on the porosity, thus the switch is explained here by a different dispersion of OBC versus WB due to their differences of shape, particles size and of compatibility with the starchy matrix (soluble versus insoluble fibers). In Exp2, for fixed fibers content, the impact of the fibers types on porosity is significant. This may be due to the nature of the matrix containing more proteins in Exp2. The switch of mechanical trends due to different porosities reflects an impact of fibers type on the ability to expand of the material, which does not exist in Exp1. This modification of the expansion ability may also arise from the morphology of the walls, depending on the fibers types (ability to be dispersed) and on the continuous matrix (ability to disperse), that may rigidify the walls upon expansion.

### 4.5. Walls structure

This level of structure of the walls is important for the understanding of the texture of such complex products. Cutting edge microscopic techniques are critical to improve our understanding of this phenomenon. The InsideFood project aimed at developing new tools for structure characterization of food products. 2D NMR relaxometry was applied to gel type products (Iuliano, Piggott, Venturi, & Hills, 2010) with a validation by microscopy. This method could give the insight needed to better understand the walls internal structure. Further developments would be needed to be able to apply this method to products such as extruded cereals with regards to the previous work performed on bread (Bosmans et al., 2012). The moisture level in the cereal would have to be increased to be able to get a decent signal. A validation with microscopic observations and quantification would be necessary. This would be an interesting but a very challenging piece of work.

## 5. Conclusion

This study dealing with two types of starchy extruded recipes with added fibers such as oat bran concentrate (OBC) and wheat bran (WB) showed that porosity of the cereals was the major product attribute impacting the maximal stress, i.e. hardness of the product, in accordance with the Gibson–Ashby relationship. However, it was possible to decouple the porosity from the walls impact by taking into account the composite behavior of the extruded materials, i.e. a starchy matrix dispersing fibers and proteins. This level of structure is thus of importance since it allowed improving the fit of the Gibson–Ashby relationship. On the basis of the matrix–particles behavior type of the extruded products supplemented in fibers, the impact of the fibers types on the two types of recipes was assessed for both Exp1 and Exp2. The switch of OBC trends versus WB was attributed to their ability to be dispersed, which modifies the morphology of the walls. Within the InsideFood project, this level of structure has been studied by 2D NMR relaxometry for highly hydrated food products such as gels. The application of this method to extruded cereals in a hydrated manner would be of interest for the food industry, since microscopy methods such as confocal scanning light microscopy are time-consuming and most of the time, the images are difficult to quantify. If the tools to quantify the structure at the solid foam level have strongly evolved within the last 10 years with the X-ray tomography development and the use of algorithms for 3D image analysis, a spectroscopic method would definitely give a quicker and interesting insight at the level of walls morphology. The 3D X-ray microscopy would also be a future method to explore for complex products such as extruded cereals. With this recent method, the different phases in the cells walls may become accessible without too much samples preparation.

## Acknowledgments

The EU (project InsideFood FP7-226783) is acknowledged for financial support. The opinions expressed in this document do by no means reflect the official opinion of the EC or of its representatives. We thank all the team members of the InsideFood project for the collaboration: K.U. Leuven, Brücker MicroCT, IFR, VCBT, VSG3D, UPM, PoliMi, Recendt, SGGW, Chaber S.A. The pilot plant operators of PTC Orbe and the apprentice Damien Testori are also acknowledged for their technical support for the production of the samples and texture analysis, respectively.

## References

Ajji, A., & Utracki, L. A. (2002). Interphase and compatibilization of polymer blends. *Polymer Engineering and Science*, *36*(12), 1574–1585.

Avérous, L. (2004). Biodegradable multiphase systems based on plasticized starch: a review. *Journal of Macromolecular Science Polymer Reviews*, *44*(3), 231–274.

Avérous, L., & Boquillon, N. (2004). Biocomposites based on plasticized starch: thermal and mechanical behaviours. *Carbohydrate Polymers*, *56*(2), 111–122.

Babin, P., Della Valle, G., Dendievel, R., Lourdin, D., & Salvo, L. (2007). X-ray tomography study of the cellular structure of extruded starches and its relations with expansion phenomenon and foam mechanical properties. *Carbohydrate Polymers*, *68*, 329–340.

Bizot, H., Le Bail, P., Leroux, B., Davy, J., Roger, P., & Buleon, A. (1997). Calorimetric evaluation of the glass transition in hydrated, linear and branched polyhydroglucose compounds. *Carbohydrate Polymers*, *32*, 33–50.

Bosmans, G. M., Lagrain, B., Deleu, L. J., Fierens, E., Hills, B. P., & Delcour, J. A. (2012). Assignments of proton populations in dough and bread using NMR relaxometry of starch, gluten, and flour model systems. *Journal of Agricultural and Food Chemistry*, *60*(21), 5461–5470.

Brennan, M. A., Monro, J. A., & Brennan, C. S. (2008). Effect of inclusion of soluble and insoluble fibres into extruded breakfast cereal products made with reverse screw configuration. *International Journal of Food Science and Technology*, *43*, 2278–2288.

Carvalho, C. W. P., Takeiti, C. Y., Onwulata, C. I., & Pordesimo, L. O. (2010). Relative effect of particle size on the physical properties of corn meal extrudates: effect of particle size on the extrusion of corn meal. *Journal of Food Engineering*, *98*, 103–109.

Chanvrier, H., Della Valle, G., & Lourdin, D. (2006). Mechanical behaviour of corn flour and starch-zein based materials in the glassy state: a matrix–particle interprétation. *Carbohydrate Polymers*, *65*, 346–356.

Chanvrier, H., Appelqvist, I. A. M., Bird, A. R., Gilbert, E., Htoon, A., Li, Z., Lillford, P. J., Lopez-Rubio, A., Morell, M. K., & Topping, D. L. (2007). Processing of novel elevated amylose wheats: functional properties and starch digestibility of extruded products. *Journal of Agricultural and Food Chemistry*, *55*, 10248–10257.

Della Valle, G., Vergnes, B., Colonna, P., & Patria, A. (1997). Relations between rheological properties of molten starches and their expansion behaviour in extrusion. *Journal of Food Engineering*, *31*(3), 277–296.

Eslami, H., & Kamal, M. R. (2012). Elongational rheology and mechanical properties of biodegradable PLA/PBSA blends. In *Annual technical conference—ANTEC, conference proceedings* (pp. 155–158).

Fan, J. T., Mitchell, J. R., & Blanshard, J. M. V. (1994). A computer simulation of the dynamics of bubble growth and shrinkage during extrudate expansion. *Journal of Food Engineering*, *23*, 337–356.

Fisher, T. (2004). Effect of extrusion cooking on protein modification in wheat flour. *European Food Research and Technology*, *218*(2), 128–132.

Fontanet, I., Davidou, S., Dacremont, C., & Le Meste, M. (1997). Effect of water in the mechanical behaviour of extruded flat bread. *Journal of Cereal Science*, *25*(3), 303–311.

Gibson, L. J., & Ashby, M. F. (1997). *Cellular solids* (2nd ed.). Cambridge, UK: Cambridge University Press.

Guessasma, S., Babin, P., Della Valle, G., & Dendievel, R. (2008). Relating cellular structure of open solid food foams to their Young's modulus: finite element calculation. *International Journal of Solids and Structures*, *45*(10), 2881–2896.

Guessasma, S., Chaunier, L., & Lourdin, D. (2010). Finite élément modelling of the mechanical behaviour of vitreous starch/protein composite. *Journal of Food Engineering*, *98*(2), 150–158.

Guessasma, S., Chaunier, L., Della Valle, G., & Lourdin, D. (2011). Mechanical modelling of cereal solid foods. *Trends in Food Science and Technology*, *22*, 142–153.

Habeych, E., Dekkers, B., van der Goot, A. J., & Boom, R. (2008). Starch-zein blends formed by shear flow. *Chemical Engineering Science*, *63*, 5229–5238.

Hedjazi, L., Guessasma, S., Della Valle, G., & Benseddiq, N. (2011). Finite element modelling of crack propagation in carbohydrate extruded starch with open void structure. *Carbohydrate Polymers*, *83*, 1696–1706.

Iuliano, C., Piggott, R. B., Venturi, L., & Hills, B. P. (2010). A two-dimensional relaxation study of the evolving microstructure in a mixed biopolymer gel. *Applied Magnetic Resonance*, *38*(3), 307–320.

Kastner, J., Kickinger, R., & Salaberger, D. (2011). High-resolution X-ray computer tomography for 3D microstructure characterization of a cellulose particle filled polymer foam. *Journal of Cellular Plastics*, *47*(6), 567–578.

Launay, G. (1994). Expansion des matériaux amylacés en sortie de filière: caractérisation expérimentales et interprétations La Cuisson-Extrusion, Tech et Doc, Paris. pp. 165–202.

Leclair, A., & Favis, B. D. (1996). The role of interfacial contact in immiscible binary polymer blends and its influence on mechanical properties. *Polymer*, *37*(21), 4723–4728.

Lourdin, D., Della Valle, G., & Colonna, P. (1995). Influence of amylose content on starch films and foam. *Carbohydrate Polymers*, *27*, 261–270.

Liu, Z., & Scanlon, M. G. (2003). Scaling Young's modulus of cellular solids. *Journal of Material Science Letters*, *22*, 547–548.

Mazzola, L., Bemporad, E., Squeo, E. A., Trovalusci, F., & Tagliaferri, V. (2011). Filler-matrix interaction in solid-state foaming of composite foams. *Journal of Cellular Plastics*, *47*(1), 31–43.

Murphy, N., Norat, T., Ferrari, P., Jenab, M., Bueno-de-Mesquita, B., Skeie, G., Dahm, C. C., & Riboli, E. (2012). Dietary fiber intake and risks of cancers of the colon and rectum in the European prospective investigation into cancer and nutrition (EPIC). *PLoS ONE*, *7*(6), art. N° e39361.

Nicholls, R. J., Appelqvist, I. A. M., Davies, A. P., Ingman, S. J., & Lillford, P. J. (1995). Glass transitions and fracture behavior of gluten and starch within the glass state. *Journal of Cereal Science*, *21*, 25–36.

Nicolais, L., & Nicomedo, L. (1974). Effect of particles shape on tensile properties of glassy thermoplastic composites. *International Journal of Polymeric Materials*, *3*(3), 229–243.

Pai, D. A., Blake, O. A., Hamaker, B. R., & Campanella, O. H. (2009). Importance of extensional rheological properties on fiber-enriched corn extrudates. *Journal of Cereal Science*, *50*, 227–234.

Robin, F., Dubois, C., Pineau, N., Schuchmann, H. P., & Palzer, S. (2011). Expansion mechanism of extruded foams supplemented with wheat bran. *Journal of Food Engineering*, *107*, 80–89.

Robin, F., Dubois, C., Curti, D., Schuchmann, H. P., & Palzer, S. (2011). Effect of wheat bran on the mechanical properties of extruded starchy foams. *Food Research International*, *44*, 2880–2888.

Robin, F., Dattinger, S., Boire, A., Forny, L., Horvat, M., Schuchmann, H. P., & Palzer, S. (2012). Elastic properties of extruded starchy melts containing wheat bran using on-line rheology and dynamic mechanical thermal analysis. *Journal of Food Engineering*, *109*(3), 414–423.
Roudaut, G., Dacremont, C., & Le Meste, M. (1998). Influence of water on the crispness of cereal-based foods: acoustic, mechanical and sensory studies. *Journal of Texture Studies*, *29*, 199–213.
Roudaut, G., Dacremont, C., Vallès Pamies, B., Colas, B., & Le Meste, M. (2002). Crispness: a critical review on sensory and material science approaches. *Trends in Food Science and Technology*, *13*, 217–227.
Sauvageot, F., & Blond, G. (1991). Effect of water activity on crispness of breakfast cereals. *Journal of Texture Studies*, *22*, 423–442.
Topping, D. (2007). Cereal complex carbohydrates and their contribution to human health. *Journal of Cereal Science*, *46*(3), 220–229.
Tosh, S. M., Brummer, Y., Miller, S., Regand, A., Defelice, C., Duss, R., Wolever, T. M. S., & Wood, P. J. (2010). Processing affects the physicochemical properties of β-glucan in oat bran cereal. *Journal of Agricultural and Food Chemistry*, *58*, 7723–7730.
Utracki, L. A. (2002). Compatibilization of polymer blends. *Canadian Journal of Chemical Engineering*, *80*(6), 1008–1016.
Vitaglione, P., Napolitano, A., & Fogliano, V. (2008). Cereal dietary fibre: a natural functional ingredient to deliver phenolic compounds into the gut. *Trends in Food Science and Technology*, *19*, 451–463.
Valles Pamies, B., Roudaut, G., Dacremont, C., Le Meste, M., & Mitchell, J. R. (2000). Understanding the texture of low moisture cereal products: mechanical and sensory measurements of crispness. *Journal of the Science of Food and Agriculture*, *80*(11), 1679–1685.
Warburton, S. C., Donald, A. M., & Smith, A. C. (1990). The deformation of brittle starch foams. *Journal of Material Science*, *27*, 1469–1474.
Xanthos, M. (2005). Functional filler for plastics. In M. Xanthos (Ed.), *Modification of polymer mechanical and rheological properties with functional filler* (pp. 17–38). Weinheim: Wiley.
Yanniotis, S., Petraki, A., & Soumpasi, E. (2007). Effect of pectin and wheat fibers on quality attributes of extruded cornstarch. *Journal of Food Engineering*, *80*, 594–599.
Yu, L., Ramaswamy, H. S., & Boye, J. (2013). Protein rich extruded products prepared from soy protein isolate–corn flour blends. *LWT Food Science and Technology*, *50*(1), 279–289.
Yao, N., Jannink, J.-L., Alavi, S., & White, P. J. (2006). Physical and sensory characteristics of extruded products made from two oat lines with different β-glucan concentrations. *Cereal Chemistry*, *83*(6), 692–699.
Zeng, M., Huang, Y., Lu, L., Fan, L., Mangavel, C., & Lourdin, C. (2011). Mechanical properties of thermo-moulded biofilms in relation to proteins/starch interactions. *Food Biophysics*, *6*, 49–57.

## Glossary

*CF:* corn flour
*Db:* dry basis
*Exp1:* experimental Design 1
*Exp2:* experimental Design 2
*F:* fibers
*MCS:* mean cells size
*MWT:* mean walls thickness
*OBC:* oat bran concentrate
*TDF:* total dietary fibers
*WB:* wheat bran
*WG:* whole grain flour